European Journal of Medicinal Chemistry 69 (2013) 872–880

Contents lists available at ScienceDirect

European Journal of Medicinal Chemistry

journal homepage: http://www.elsevier.com/locate/ejmech

Preliminary communication

Flavones as isosteres of 4(1*H*)-quinolones: Discovery of ligand efficient and dual stage antimalarial lead compounds

Tiago Rodrigues [a, *, 1], Ana S. Ressurreição [a, 1], Filipa P. da Cruz [b], Inês S. Albuquerque [b], Jiri Gut [c], Marta P. Carrasco [a], Daniel Gonçalves [a], Rita C. Guedes [a], Daniel J.V.A. dos Santos [a, d], Maria M. Mota [b], Philip J. Rosenthal [c], Rui Moreira [a], Miguel Prudêncio [b], Francisca Lopes [a]

[a] *Research Institute for Medicines and Pharmaceutical Sciences (iMed.UL), Faculty of Pharmacy, University of Lisbon, Av. Prof. Gama Pinto, 1649-019 Lisbon, Portugal*
[b] *Instituto de Medicina Molecular, Faculdade de Medicina, Universidade de Lisboa, Av. Prof. Egas Moniz, 1649-028 Lisboa, Portugal*
[c] *Department of Medicine, San Francisco General Hospital, University of California, San Francisco, Box 0811, San Francisco, CA 94143, USA*
[d] *REQUIMTE, Department of Chemistry & Biochemistry, Faculty of Sciences, University of Porto, R. do Campo Alegre, 4169-007 Porto, Portugal*

ARTICLE INFO

Article history:
Received 14 July 2013
Received in revised form
1 September 2013
Accepted 3 September 2013
Available online 20 September 2013

Keywords:
Malaria
Flavone
Ligand efficiency
Dual stage inhibitor

ABSTRACT

Malaria is responsible for nearly one million deaths annually, and the increasing prevalence of multi-resistant strains of *Plasmodium falciparum* poses a great challenge to controlling the disease. A diverse set of flavones, isosteric to 4(1*H*)-quinolones, were prepared and profiled for their antiplasmodial activity against the blood stage of *P. falciparum* W2 strain, and the liver stage of the rodent parasite *Plasmodium berghei*. Ligand efficient leads were identified as dual stage antimalarials, suggesting that scaffold optimization may afford potent antiplasmodial compounds.

1. Introduction

The success of drug discovery programs relies heavily on innovation, in particular on the design of new chemical entities capable of modulating drug target functions [1]. This is especially true in the case of malaria, which remains the world's top-priority tropical disease due to its high mortality and morbidity. The emergence and spread of multidrug-resistant *Plasmodium falciparum*, the most virulent human malaria parasite, is still a major obstacle in controlling malaria [2]. Most currently used drugs act against the parasite forms that invade erythrocytes and cause malarial symptoms [3]. However, the parasite's life cycle in the human host also includes an asymptomatic, and obligatory developmental phase in the liver, where exo-erythrocytic forms (EEFs) develop in hepatocytes prior to bloodstream infection [4]. The life cycles of two other human malaria parasites, *Plasmodium vivax* and *Plasmodium ovale*, also include hypnozoites, which persist in the liver for long periods of time, and can cause relapses after successful clearance of bloodstream infections. Primaquine (**1**, Fig. 1) is the only available drug to treat hypnozoites of *P. vivax* and *P. ovale*, but its use is limited due to toxic effects [5,6]. Recently, efforts have focused on discovering safer drug candidates capable of blocking the development of the malarial liver stage [7–9], and of eliminating hypnozoites [10–12]. For example, 4(1*H*)-quinolones and analogs are highly effective against erythrocytic forms and EEFs of *Plasmodium* spp. [13–19]. Most commonly, cytochrome bc_1 is the main drug target for these compounds [20,21], but in some cases, such as **2** and **3** (Fig. 1), NADH:ubiquinone oxidoreductase (PfNDH2) is also blocked [17,22]. Docking studies using a crystal structure of the bc_1 complex from *Saccharomyces cerevisiae* suggest that 4(1*H*)-quinolones bind to the Q_o site of cytochrome *b* with a pose similar to that of stigmatellin, (**4**, Fig. 1). Key interactions in this binding model are the H-bond bridges with Glu^{272} and His^{181} (from the Rieske iron–

Abbreviations: CQ, chloroquine; DBU, 1,8-diazabicycloundec-7-ene; DMF, *N*, *N*-dimethylformamide; EEF, exo-erythrocytic form; *LE*, ligand efficiency; NBS, *N*-bromosuccinimide; PfNDH2, *Plasmodium falciparum* NADH:ubiquinone oxidoreductase; SAR, structure–activity relationships.

* Corresponding author. Present address: ETH Zürich, Institute of Pharmaceutical Sciences, Wolfgang-Pauli-Str. 10, 8093 Zürich, Switzerland. Tel.: +41 44 633 91 13.
E-mail address: tiago.rodrigues@pharma.ethz.ch (T. Rodrigues).

[1] T.R. and A.S.R. contributed equally to this work.

0223-5234/$ – see front matter © 2013 Elsevier Masson SAS. All rights reserved.
http://dx.doi.org/10.1016/j.ejmech.2013.09.008

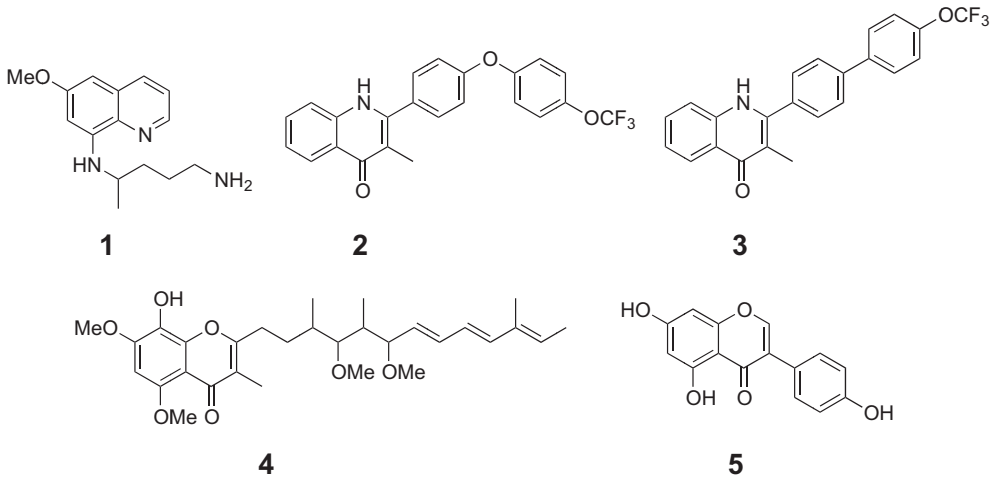

Fig. 1. Structures of antimalarial compounds **1**–**5**.

sulfur protein) [15,22]. Thus, flavones isosteric with quinolones **2** and **3** could provide further insight into the molecular basis of cytochrome bc_1 inhibition, since the endocyclic oxygen atom can only interact as a hydrogen bond acceptor, in contrast to the quinolone NH. While flavones have shown activity against blood stages of *P. falciparum* [23–25], their activity against the liver stage of malaria parasites has not yet been reported, except for the related isoflavone genistein (**5**, Fig. 1) [26]. Hence, to assess the potential of the aforementioned scaffold as a 2-aryl-4(1*H*)-quinolone isostere, we now report the synthesis and dual stage antiplasmodial activity of a diverse set of synthetic flavones.

2. Results and discussion

2.1. Molecular modeling

The structure–activity relationships (SAR) of known bc_1 complex inhibitors were taken into account for the design of compounds **6** [17,27–29]. For example, diaryl ether and biphenyl side chains were shown appropriate for maintaining a high overall lipophilicity [30] and occupying the hydrophobic Q_o pocket. In order to evaluate the potential of hydrophobic flavones as bc_1 complex inhibitors we performed a docking study using the homologous enzyme from *S. cerevisiae* as previously described [31]. In the absence of a crystallographic structure for the bc_1 complex of *P. falciparum*, much of the key structural and mechanistic information has been derived from the yeast bc_1 system, which shows high sequence identity to the *P. falciparum* orthologous enzyme [32]. 4(1*H*)-Quinolone **2** was first docked into the Q_o active site of the *S. cerevisiae* bc_1 complex (PDB code 3CX5 [33]). Several flavones containing chemically distinct side chains were also modeled and compared with compound **2** in terms of binding pose and free energy. Superposition of the binding poses obtained for **2**, **6a** and **6q** suggests that flavones and 4(1*H*)-quinolones may exert similar interactions within the Q_o site (Fig. 2A). The aromatic core of both classes of inhibitors most likely occupies the same part of the pocket. More specifically, in this model, the binding modes of **2** and **6a** are comparable, as both may interact with the protonated His^{181} residue – 2.4 or 3.1 Å, respectively (Fig. 2B). Strong interactions with His^{181} are considered of extreme importance for Q_o site inhibition since this residue is coordinated to the Rieske iron–sulfur protein, an extremely mobile subunit of the bc_1 complex with recognized significance for electron transfer and, therefore, for functional activity [34,35]. In the case of **2**, reported models suggest a water-mediated hydrogen bond between the NH group of the quinolone ring and Glu^{272}, a highly conserved residue [36]. For flavones in general, this kind of interaction may be missing since they do not contain a hydrogen-bond donor. However, when considering the most favorable pose obtained for **2** and flavone **6a**, both inhibitors display binding free energy values in the same range, −9.95 kcal/mol and −10.12 kcal/mol, respectively. As previously reported, these results suggest the importance of hydrophobic interactions for bc_1 complex inhibition [37]. Also, the comparable binding poses suggest that these two classes of compounds may share the same mechanism of action against *P. falciparum*.

2.2. Chemistry

We synthesized a small library of decorated flavones, **6a**–**r**, with the main purpose of probing chemical space. The backbone for the required side chains was acquired from condensation of 4-fluorobenzonitrile, **7**, with diverse hydroxyl-containing building blocks (Scheme 1A). Subsequently, nitriles **8a**–**d** were converted in H_2O_2 [38] to the corresponding carboxylic acids, **9a**–**d**, in excellent

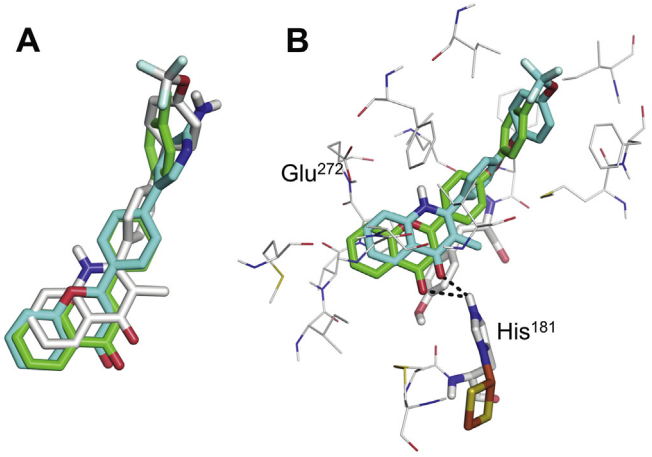

Fig. 2. (A) Superposition of the most favorable docked poses of compound **2** (carbon atoms in gray) and flavones **6a** (carbon atoms in green) and **6q** (carbon atoms in blue); (B) Predicted binding poses for quinolone **2** (carbon atoms in blue) and flavone **6a** (carbon atoms in green). (For interpretation of the references to color in this figure legend, the reader is referred to the web version of this article.)

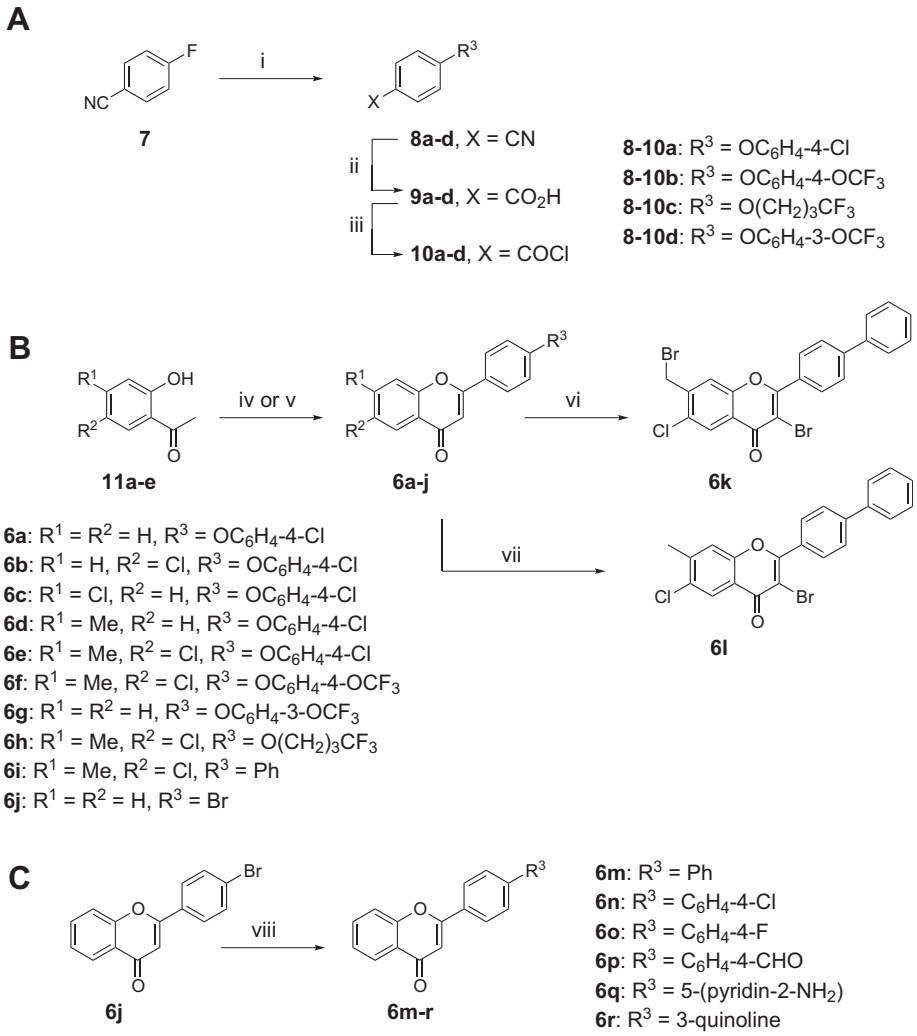

Scheme 1. Synthesis of flavone derivatives **6a**–**r**. Reagents and conditions: (i) phenol or alcohol, DMF, Na_2CO_3, reflux; (ii) EtOH, MeOH, KOH, H_2O_2, reflux; (iii) $SOCl_2$, reflux; (iv) pyridine, **9a**–**d**, DBU, reflux; (v) pyridine, **9a**–**d**, DBU, MW, 150 °C; (vi) **6i**, NBS, CCl_4, benzoyl peroxide, reflux; (vii) **6i**, NBS, $ZrCl_4$, CCl_4, rt; (viii) $R^3B(OH)_2$, $PdCl_2(Ph_3P)_2$, Na_2CO_3 1 N, dioxane, 100 °C.

yields, which were converted to their acid chlorides **10a**–**d** counterparts by reaction with $SOCl_2$. The acid chlorides were used without purification to obtain flavones **6a**–**j**, isosteric to **2** and **3**, in a one-pot Baker–Venkataraman procedure [39]. The protocol consisted of refluxing suitable acid chloride derivatives and the required 2-hydroxyacetophenones in dry pyridine and DBU for 24 h. Compounds **6a**–**j** were obtained in moderate overall yields (11–37% for a total of 4 steps) (Scheme 1B). The same procedure was reproduced in microwaves at 150 W, 150 °C for 40 min to afford flavones in comparable yields. The identification of a key singlet at *ca.* δ 6.8 ppm for H-3 in the ^{1}H NMR spectrum confirmed the final cyclization step. Bromination of **6i** was performed using NBS and benzoyl peroxide or $ZrCl_4$ [40] to give **6k** and **6l** (Scheme 1B). Finally, we expanded the diversity at the aryl moiety in ring B, by performing Suzuki coupling reactions with the 2-(4-bromophenyl) flavone **6j** and appropriate boronic acids to give compounds **6m**–**r**, which are isosteric with **3**, in 42–82% yield (Scheme 1C).

2.3. *In vitro* antiplasmodial activity

The in vitro antiplasmodial activity of compounds **6** was evaluated against the chloroquine-resistant *P. falciparum* W2 strain (Table 1), according to the procedure described by Semenov et al. [41]. All compounds exhibited moderate antiplasmodial activity, in the range reported for other flavones [23,42]. Inspection of data in Table 1 shows that derivative **6k**, with an IC_{50} value of *ca.* 6 μM, is at least 4 times more active than its 7-methyl counterpart **6l**. Replacement of the 4-phenyl group at ring B by a 4-aryloxy moiety has a detrimental effect on antiplasmodial activity (**6i** *vs.* **6e** and **6f**), but a 4-(2′-trifluoropropoxy) moiety, **6h**, affords a compound equipotent to **6g**.

On the other hand, flavones containing a basic group at the 4-phenyl moiety in ring B, **6q** and **6r**, displayed improved activity when compared to their non-basic counterparts **6m-p**. In particular, the antiplasmodial potency displayed by **6q** may be driven by the lowest *c*log *P* value among series **6** (Table 1). With the exception of **6q**, these flavones present high *c*log *P* values and low aqueous solubility that may lead to poor cell permeability and explain the IC_{50} values against the W2 strain.

Ligand efficiency (*LE*) is a useful metric to prioritize hits and guide hit-to-lead optimization efforts. Irrespective of IC_{50} values, compounds showing $LE \geq 0.30$ are generally accepted as good starting points for optimization [43–45]. In that regard, **6q** meets the requirements of an early lead ($LE = 0.32$), with the added value of presenting low molecular weight. Thus, **6q** provides ample opportunity for medicinal chemistry.

Table 1
Antiplasmodial activity of flavones **6a**–**r** against *P. falciparum* W2 strain and their calculated molecular properties.[a]

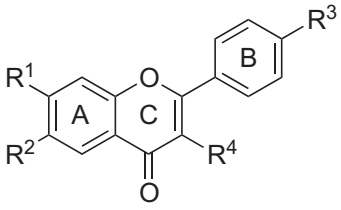

Cpd.	R^1	R^2	R^3	R^4	$IC_{50} \pm SD$ (μM)	clog *P*	log *S*	MW	*LE*[b]
6a	H	H	OC_6H_4-4-Cl	H	21.0 ± 0.37	5.62	−6.78	358	0.26
6b	H	Cl	OC_6H_4-4-Cl	H	>25.0	6.23	−7.51	382	ND
6c	Cl	H	OC_6H_4-4-Cl	H	12.6 ± 0.25	6.23	−7.51	382	0.26
6d	Me	H	OC_6H_4-4-Cl	H	19.7 ± 2.98	5.93	−7.12	362	0.25
6e	Me	Cl	OC_6H_4-4-Cl	H	23.2 ± 0.11	6.54	−7.86	396	0.24
6f	Me	Cl	OC_6H_4-4-OCF_3	H	>25.0	6.76	−8.14	446	ND
6g	H	H	OC_6H_4-3-OCF_3	H	14.9 ± 1.20	5.83	−7.06	398	0.23
6h	Me	Cl	$O(CH_2)_3CF_3$	H	17.2 ± 0.86	5.80	−6.15	382	0.26
6i	Me	Cl	Ph	H	14.0 ± 0.59	6.20	−6.91	346	0.27
6j	H	H	Br	H	>25.0	4.29	−4.58	300	ND
6k	CH_2Br	Cl	Ph	Br	5.96 ± 0.07	6.96	−8.66	502	0.27
6l	Me	Cl	Ph	Br	>25.0	6.66	−7.74	424	ND
6m	H	H	Ph	H	>25.0	5.27	−5.83	298	ND
6n	H	H	C_6H_4-4-Cl	H	>10.0	5.89	−6.57	332	ND
6o	H	H	C_6H_4-4-F	H	>25.0	5.33	−6.14	316	ND
6p	H	H	C_6H_4-4-CHO	H	>25.0	4.96	−6.15	326	ND
6q	H	H	5-(Pyridin-2-NH_2)	H	3.88 ± 0.37	3.95	−5.64	313	0.32
6r	H	H	3-Quinoline	H	5.17 ± 0.10	5.59	−6.54	349	0.27
CQ					0.186 ± 0.060	4.37	−4.06	319	0.47

[a] Molecular properties were calculated using the OSIRIS property explorer (http://www.organic-chemistry.org/prog/peo/).
[b] Whole cell (W2 strain) ligand efficiency [$LE = -1.4 \bullet \log(IC_{50})/HA$, where HA = number heavy atoms]; CQ – chloroquine; ND – not determined.

Based on the reported activity of genistein against *Plasmodium* liver stages (IC_{50} *ca.* 20 μM) [26], flavones **6** were also evaluated for dual stage activity, by assessing their ability to inhibit development of *Plasmodium berghei* sporozoites in human hepatoma Huh-7 cells [46]. The results presented in Fig. 3 show that compounds **6a**–**r** decreased the infection load of Huh-7 cells to different extents when compared to untreated controls. IC_{50} values were determined for flavones **6a**, **6d**, **6i** and **6q**, which were the most potent inhibitors in the preliminary two-concentration screen (Fig. 3). Compound **6q** presented an IC_{50} value of 1.9 μM and favorable ligand efficiency (*LE* = 0.33). On the other hand, **6i** presented an IC_{50} value of 8.5 μM, while **6a** and **6d** displayed IC_{50} values of 6.2 μM and 4.1 μM, respectively. Interestingly, potency against the liver stage does not correlate with that against erythrocytic-stage parasites. These results suggest (i) different drug targets for different stages of the life cycle and (ii) the value of flavones as ligand efficient leads for liver stage malaria (Table 2). Additionally, our data suggests that most of the promising compounds had no significant cytotoxicity at assayed concentrations.

3. Conclusions

In summary, a small library of flavones isosteric to 4(1*H*)-quinolones was synthesized and profiled against blood and liver stage malaria. Our preliminary studies identified ligand efficient compounds as dual stage antimalarials. In particular, **6q** presents physicochemical properties in the lead-like chemical space, providing ample opportunity for medicinal chemistry optimization. To the best of our knowledge this is the first report of synthetic flavones with activity against the liver stage of malaria parasites, against which new drugs are urgently sought. In addition, the results herein reported are consistent with the current binding model of bc_1 Q_o inhibitors, highlighting the importance of the interactions with Glu^{272} and His^{181} for optimal activity.

4. Experimental section

4.1. Chemistry

Flash chromatography was performed on Kieselgel 60 GF254 silica (Merck) of 0.040–0.063 mm. Thin layer chromatography (TLC) was performed on aluminum sheets with silica gel F250 (Merck) and visualized under UV light or by exposure to iodine vapor. All reactions were monitored by TLC. Melting points were determined using a Kofler camera Bock Monoscope M and are uncorrected. The IR spectra were determined as films on a Nicolet Impact 400 FTIR spectrophotometer, and only the most significant absorption bands are reported. Low-resolution mass spectra (MS) were recorded using a VG Quattro LCMS instrument. High-resolution mass spectra (HRMS) were performed on a Bruker MicrOTOF equipped with ESI ion source from the Mass Spectrometry and Proteomics Unity of the University of Santiago de Compostela, Spain. Elemental analyses were performed using an EA 1110 CE Instruments automatic analyzer. The NMR spectra were recorded on a Bruker Avance 400 NMR spectrometer (^1H, 400 MHz; ^{13}C, 101 MHz). ^1H and ^{13}C chemical shifts, δ, are expressed in ppm (parts per million) with the solvent signal as internal standard [$CDCl_3$: δ (^1H) 7.26 ppm and δ (^{13}C) 77.2 ppm]. Coupling constants

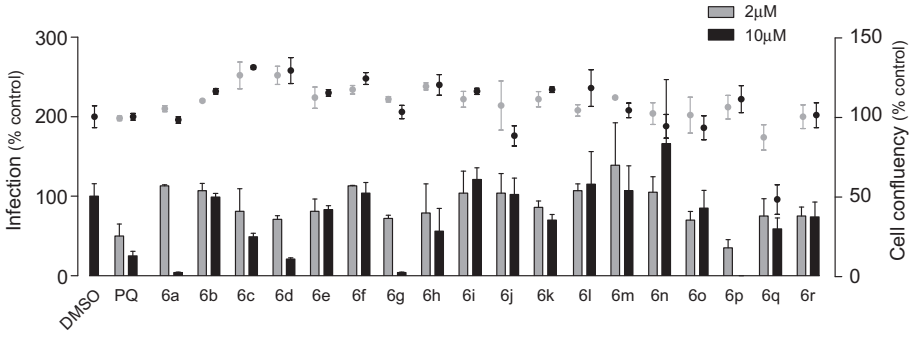

Fig. 3. Antiplasmodial activity of compounds **6** against the liver stage of *P. berghei*. The luminescence (bars) measures the extent of *Plasmodium* hepatic infection and is given as percentage of the infection of solvent-treated control cells. Cell confluency was determined by fluorescence (dots) following incubation with AlamarBlue, and is also given as percentage of solvent-treated control cells. Compounds **6** and primaquine were tested at two concentrations (10 μM and 2 μM). Control – Cells incubated with an amount of DMSO equivalent to that used in the highest compound concentrations.

Table 2
Antiplasmodial activity of **6a**, **6d**, **6i** and **6q** against *P. berghei* liver stage.

Compound	IC_{50} (μM)	*LE*[a]	CC_{50} (μM)
6a	6.2	0.30	>180
6d	4.1	0.30	>50
6i	8.5	0.28	>90
6q	1.9	0.33	>15
Genistein	20	0.33	ND
Primaquine	7.5	0.38	ND

[a] Ligand efficiency (*LE*) based on whole cell assay (Huh-7 cells infected with *P. berghei* sporozoites); ND – not determined.

(*J*) are reported in Hertz (Hz). The microwave-assisted synthesis was performed in a CEM Corporation Discover® Labmate™.

*4.1.1. General procedure for the preparation of 4-phenoxybenzonitriles (**8a–d**)*

A suitable phenol or alcohol (1 M eq.), 4-fluorobenzonitrile (1 M eq.) and Na_2CO_3 (2 M eq.) were suspended in DMF (3.5 mL/mmol) and heated. The reaction was followed by TLC, hexane:diethyl ether (9:1), and after completion (approximately 24 h), the desired product extracted with CH_2Cl_2 (3 × 50 mL). The crude product was purified by flash chromatography, using hexane:diethyl ether (100:1) as eluent.

*4.1.1.1. 4-(4-Chlorophenoxy)benzonitrile (**8a**).* White solid; 100%; mp 67–68 °C; ^{1}H NMR ($CDCl_3$, 400 MHz) δ 7.01–7.04 (4H, m, Ar–*H*); 7.40 (2H, d, *J* = 6.8 Hz, Ar–*H*); 7.63 (2H, d, *J* = 6.8 Hz, Ar–*H*).

*4.1.1.2. 4-(4-(Trifluoromethoxy)phenoxy)benzonitrile (**8b**).* Yellow oil; 100%; ^{1}H NMR ($CDCl_3$, 400 MHz) δ 7.04 (2H, d, *J* = 9.0 Hz, Ar–*H*); 7.11 (2H, d, *J* = 9.0 Hz, Ar–*H*); 7.28 (2H, d, *J* = 9.0 Hz, Ar–*H*); 7.64 (2H, d, *J* = 9.0 Hz, Ar–*H*).

*4.1.1.3. 4-(4,4,4-Trifluorobutoxy)benzonitrile (**8c**).* Transparent oil; 94%; ^{1}H NMR ($CDCl_3$, 400 MHz) δ 2.12 (2H, m, $CH_2CH_2CH_2$); 2.35 (2H, m, $CH_2CH_2CF_3$); 4.09 (2H, t, *J* = 6.0 Hz, $CH_2CH_2CH_2CF_3$); 6.96 (2H, d, *J* = 8.4 Hz, Ar–*H*); 7.62 (2H, d, *J* = 8.4 Hz, Ar–*H*).

*4.1.1.4. 4-(3-(Trifluoromethoxy)phenoxy)benzonitrile (**8d**).* Yellow oil; 100%; ^{1}H NMR ($CDCl_3$, 400 MHz) δ 6.97 (1H, br. s, Ar–*H*); 7.02 (1H, dd, *J* = 8.6 and 2.0 Hz, Ar–*H*); 7.05–7.14 (3H, m, Ar–*H*); 7.45 (1H, t, *J* = 8.2 Hz, Ar–*H*); 7.67 (2H, d, *J* = 9.0 Hz, Ar–*H*).

*4.1.2. General procedure for the preparation of 4-phenoxybenzoic acids (**9a–d**) [47]*

Benzonitrile (1 M eq.) and KOH in pellets (18 M eq.) were suspended in MeOH (0.6 mL/mmol), and EtOH (2.6 mL/mmol). H_2O_2 30% (1.0 mL/mmol) was added dropwise to avoid rapid heating and effervescence. After heating to reflux temperature, for 4 h, the reaction mixture was acidified with concentrated HCl, and the solid extracted with CH_2Cl_2 (3 × 20 mL) to afford the required compound.

*4.1.2.1. 4-(4-Chlorophenoxy)benzoic acid (**9a**).* White solid; 100%; mp 150–152 °C; ^{1}H NMR ($CDCl_3$, 400 MHz) δ 7.02–7.06 (4H, m, Ar–*H*); 7.39 (2H, d, *J* = 6.8 Hz, Ar–*H*); 8.10 (2H, d, *J* = 6.8 Hz, Ar–*H*).

*4.1.2.2. 4-(4-(Trifluoromethoxy)phenoxy)benzoic acid (**9b**).* White needles; 98%; mp 141–143 °C; ^{1}H NMR ($CDCl_3$, 400 MHz) δ 7.05 (2H, d, *J* = 6.8 Hz, Ar–*H*); 7.12 (2H, d, *J* = 6.8 Hz, Ar–*H*); 7.28 (2H, d, *J* = 6.8 Hz, Ar–*H*); 8.12 (2H, d, *J* = 6.8 Hz, Ar–*H*).

*4.1.2.3. 4-(4,4,4-Trifluorobutoxy)benzoic acid (**9c**).* Pinkish solid; 95%; mp 97–99 °C; ^{1}H NMR ($CDCl_3$, 400 MHz) δ 2.12 (2H, m, $CH_2CH_2CH_2$); 2.35 (2H, m, $CH_2CH_2CF_3$); 4.09 (2H, t, *J* = 6.0 Hz, $CH_2CH_2CH_2CF_3$); 6.96 (2H, d, *J* = 8.4 Hz, Ar–*H*); 7.62 (2H, d, *J* = 8.4 Hz, Ar–*H*).

*4.1.2.4. 4-(3-(Trifluoromethoxy)phenoxy)benzoic acid (**9d**).* Yellow gum; 96%; ^{1}H NMR ($CDCl_3$, 400 MHz) δ 6.98 (1H, br. s, Ar–*H*); 7.03 (1H, dd, *J* = 8.2 and 2.0 Hz, Ar–*H*); 7.04–7.10 (3H, m, Ar–*H*); 7.43 (1H, t, *J* = 8.2 Hz, Ar–*H*); 8.13 (2H, d, *J* = 9.0 Hz, Ar–*H*).

*4.1.3. General procedure for the preparation of flavones **6a–i***

The benzoic acids **9a–d** (1 M eq.) were refluxed with $SOCl_2$ (3 mL/mmol) for 24 h. The solvent was evaporated and the acid chlorides **10a–d** were used without further purification. DBU (2.2 M eq.) was added to a solution of 2-hydroxyacetophenone (2 M eq.) and benzoyl chloride (1 M eq.) in dry pyridine (4 mL/mmol). The mixture was stirred for 6–24 h at reflux, cooled to room temperature and poured into HCl 1 N (20–25 mL), containing ice. The solution was extracted with CH_2Cl_2 (3 × 50 mL), the combined extracts were dried upon Na_2SO_4 and evaporated to dryness *in vacuum*. The crude product was purified by flash chromatography eluting with hexane:EtOAc (9:1).

*4.1.3.1. 2-(4-(4-Chlorophenoxy)phenyl)-4H-chromen-4-one (**6a**).* Pale yellow solid; 30%; mp 132–133 °C; ^{1}H NMR ($CDCl_3$, 400 MHz) δ 6.80 (1H, s, Ar–*H*3); 7.07 (2H, d, *J* = 8.8 Hz, Ar–*H*); 7.31 (2H, d, *J* = 8.8 Hz, Ar–*H*); 7.40 (2H, d, *J* = 8.8 Hz, Ar–*H*); 7.45 (1H, t, *J* = 7.2 Hz, Ar–*H*); 7.59 (1H, d, *J* = 7.2 Hz, Ar–*H*); 7.73 (1H, t, *J* = 7.2 Hz, Ar–*H*); 7.93 (2H, d, *J* = 8.8 Hz, Ar–*H*); 8.27 (1H, d, *J* = 7.2 Hz, Ar–*H*); ^{13}C NMR ($CDCl_3$, 101 MHz) δ 106.9; 118.0; 118.3; 121.2; 123.9; 125.3; 125.7; 126.5; 128.2; 129.7; 130.1; 133.8; 154.4; 156.2; 160.3; 162.9; 178.4; IR (film): ν_{max} 1638; 1472; 1402; 1364; 1243 cm^{-1}; ESI-MS *m*/*z* (abund.): 349 $[M + H]^+$ (100); Anal. Calcd. ($C_{21}H_{13}ClO_3 \cdot 0.1EtOAc$): C, 71.88; H, 3.89%. Found: C, 72.14; H, 3.76%.

*4.1.3.2. 6-Chloro-2-(4-(4-chlorophenoxy)phenyl)-4H-chromen-4-one (**6b**).* Pale yellow solid; 15%; mp 165–167 °C; ^{1}H NMR ($CDCl_3$, 400 MHz) δ 6.78 (1H, s, Ar–*H*3); 7.05 (2H, d, *J* = 8.8 Hz, Ar–*H*); 7.11 (2H, d, *J* = 8.8 Hz, Ar–*H*); 7.39 (2H, d, *J* = 8.8 Hz, Ar–*H*); 7.55 (1H, d, *J* = 8.8 Hz, Ar–*H*); 7.67 (1H, dd, *J* = 8.8 and 2.4 Hz, Ar–*H*); 7.91 (2H, d, *J* = 8.8 Hz, Ar–*H*); 8.21 (1H, d, *J* = 2.4 Hz, Ar–*H*); ^{13}C NMR ($CDCl_3$, 101 MHz) δ 106.8; 118.3; 119.7; 121.3; 124.9; 125.2; 126.0; 128.3; 129.8; 130.2; 131.2; 133.9; 154.2; 154.5; 160.6; 163.2; 177.1; IR (film): ν_{max} 1625; 1479; 1434; 1351; 1236; 824 cm^{-1}; ESI-MS *m*/*z* (abund.): 383 $[M + H]^+$ (100); Anal. Calcd. ($C_{21}H_{12}Cl_2O_3$): C, 65.82; H, 3.16%. Found: C, 66.17; H, 3.07%.

*4.1.3.3. 7-Chloro-2-(4-(4-chlorophenoxy)phenyl)-4H-chromen-4-one (**6c**).* Yellow solid; 32%; mp 179–181 °C; ^{1}H NMR ($CDCl_3$, 400 MHz) δ 6.75 (1H, s, Ar–*H*3); 7.06 (2H, d, *J* = 7.2, Ar–*H*); 7.12 (2H, d, *J* = 8.0, Ar–*H*); 7.40 (2H, d, *J* = 7.2, Ar–*H*); 7.41 (1H, dd, *J* = 8.4 and 2.0 Hz, Ar–*H*); 8.62 (1H, d, *J* = 2.0, Ar–*H*); 7.91 (2H, d, *J* = 8.0 Hz, Ar–*H*); 8.19 (1H, d, *J* = 8.4 Hz, Ar–*H*); ^{13}C NMR ($CDCl_3$, 101 MHz) δ 107.1; 118.1; 118.3; 121.3; 122.5; 126.0; 126.1; 127.1; 128.3; 129.8; 130.2; 139.8; 154.3; 156.3; 160.6; 163.2; 177.5; IR (film): ν_{max} 1645; 1479; 1415; 1364; 1242 cm^{-1}; ESI-MS *m*/*z* (abund.): 383 $[M + H]^+$ (100); Anal. Calcd. ($C_{21}H_{12}Cl_2O_3$): C, 65.82; H, 3.16%. Found: C, 65.56; H, 3.09%.

*4.1.3.4. 2-(4-(4-Chlorophenoxy)phenyl)-7-methyl-4H-chromen-4-one (**6d**).* White solid; 11%; mp 138–139 °C; ^{1}H NMR ($CDCl_3$, 400 MHz) δ 2.54 (3H, s, CH_3); 6.76 (1H, s, Ar–*H*3); 7.06 (2H, d, *J* = 7.2 Hz, Ar–*H*); 7.11 (2H, d, *J* = 7.2 Hz, Ar–*H*); 7.26 (1H, dd, *J* = 8.0 and 1.2 Hz, Ar–*H*); 7.38–7.40 (3H, m, Ar–*H*); 7.91 (2H, d, *J* = 7.2 Hz, Ar–*H*); 8.13 (1H, d, *J* = 8.0 Hz, Ar–*H*); ^{13}C NMR ($CDCl_3$, 101 MHz) δ 21.9; 106.9; 117.8; 118.3; 121.2; 121.7; 125.5; 126.6; 126.7; 128.2; 129.6; 130.1; 145.1; 154.4; 156.3; 160.2; 162.6; 178.3; IR (film): ν_{max} 1632; 1485; 1421; 1370; 1243; 827 cm^{-1}; ESI-MS *m*/*z* (abund.): 363

$[M + H]^+$ (100); Anal. Calcd. ($C_{22}H_{15}ClO_3$): C, 72.83; H, 4.17%. Found: C, 72.59; H, 4.16%.

*4.1.3.5. 6-Chloro-2-(4-(4-chlorophenoxy)phenyl)-7-methyl-4H-chromen-4-one (**6e**).* Yellow solid; 21%; mp 185–187 °C; ^{1}H NMR ($CDCl_3$, 400 MHz) δ 2.54 (3H, s, C*H*$_3$); 6.76 (1H, s, Ar–*H*3); 7.06 (2H, d, J = 7.2 Hz, Ar–*H*); 7.10 (2H, d, J = 7.2 Hz, Ar–*H*); 7.39 (2H, d, J = 7.2 Hz, Ar–*H*); 7.48 (1H, s, Ar–*H*); 7.90 (2H, d, J = 7.2 Hz, Ar–*H*); 8.20 (1H, s, Ar–*H*); ^{13}C NMR ($CDCl_3$, 101 MHz) δ 20.9; 106.7; 118.3; 119.9; 121.3; 123.0; 125.4; 126.2; 128.2; 129.7; 130.1; 131.9; 143.00; 154.3; 154.5; 160.5; 162.9; 177.2; IR (film): ν_{max} 1630; 1481; 1400; 1237; 1163; 827 cm^{-1}; ESI-MS m/z (abund.): 397 $[M + H]^+$ (100); Anal. Calcd. ($C_{22}H_{14}Cl_2O_3$+0.2H_2O): C, 65.92; H, 3.62%. Found: C, 65.72; H, 3.50%.

*4.1.3.6. 6-Chloro-7-methyl-2-(4-(4-trifluoromethoxy)phenoxy) phenyl-4H-chromen-4-one (**6f**).* Pinkish solid; 40%; mp 171–173 °C; ^{1}H NMR ($CDCl_3$, 400 MHz) δ 2.55 (3H, s, C*H*$_3$); 6.76 (1H, s, Ar–*H*3); 7.12–7.14 (4H, m, Ar–*H*); 7.28 (2H, d, J = 8.0 Hz, Ar–*H*); 7.48 (1H, s, Ar–*H*8); 7.91 (2H, d, J = 7.2 Hz, Ar–*H*); 8.20 (1H, s, Ar–*H*5); ^{13}C NMR ($CDCl_3$, 101 MHz) δ 20.9; 106.8; 118.5; 119.9; 120.9; 122.9; 122.9; 123.0; 123.0; 125.4; 126.4; 128.3; 132.0; 143.0; 145.5; 154.2; 160.3; 162.8; 177.2; IR (film): ν_{max} 1630; 1503; 1251; 1163; 1037; 904; 830 cm^{-1}; ESI-MS m/z (abund.): 447 $[M + H]^+$ (100); Anal. Calcd. ($C_{23}H_{14}ClF_3O_4$): C, 61.83; H, 3.16%. Found: C, 61.86; H, 3.10%.

*4.1.3.7. 2-([1,1′-Biphenyl]-4-yl)-6-chloro-7-methyl-4H-chromen-4-one (**6i**).* Yellow solid; 27%; mp 197–199 °C; ^{1}H NMR ($CDCl_3$, 400 MHz) δ 2.56 (3H, s, C*H*$_3$); 6.87 (1H, s, Ar–*H*3); 7.44 (1H, tt, J = 1.2 and 7.2 Hz, Ar–*H*); 7.50–7.54 (3H, m, Ar–*H* and Ar–*H*8); 7.68 (2H, d, J = 8.0 Hz, Ar–*H*); 7.78 (2H, d, J = 6.8 Hz, Ar–*H*); 8.01 (2H, d, J = 6.8 Hz, Ar–*H*); 8.22 (1H, s, Ar–*H*5); ^{13}C NMR ($CDCl_3$, 101 MHz) δ 20.9; 107.2; 120.0; 123.1; 125.4; 126.8; 127.2; 127.7; 128.3; 129.0; 129.1; 130.3; 132.0; 139.7; 143.1; 144.6; 154.5; 177.3; IR (film): ν_{max} 1630; 1451; 1407; 1244; 1051; 908; 827 cm^{-1}; ESI-MS m/z (abund.): 347 $[M + H]^+$ (100); Anal. Calcd. ($C_{22}H_{15}ClO_2 \cdot 0.2CH_2Cl_2$): C, 73.29; H, 4.27%. Found: C, 73.66; H, 4.31%.

*4.1.3.8. 6-Chloro-7-methyl-2-(4-(4,4,4-trifluorobutoxy)phenyl)-4H-chromen-4-one (**6h**).* Yellow solid; 15%; mp 161–162 °C; ^{1}H NMR ($CDCl_3$, 400 MHz) δ 2.13 (2H, m, $CH_2CH_2CH_2$); 2.36 (2H, m, $CH_2CH_2CF_3$); 2.54 (3H, s, C*H*$_3$); 4.13 (2H, t, J = 6.0 Hz, $CH_2CH_2CH_2CF_3$); 6.74 (1H, s, Ar–*H*3); 7.03 (2H, d, J = 8.6 Hz, Ar–*H*); 7.48 (1H, s, Ar–*H*8); 7.88 (2H, d, J = 8.6 Hz, Ar–*H*); 8.19 (1H, s, Ar–*H*5); ^{13}C NMR ($CDCl_3$, 101 MHz) δ 20.9; 22.1; 29.8; 30.5; 66.3; 106.1; 114.9; 119.9; 123.0; 124.2; 125.4; 128.1; 131.8; 142.8; 154.5; 161.4; 163.4; 177.2; IR (film): ν_{max} 1638; 1504; 1408; 1243; 1019 cm^{-1}; ESI-MS m/z (abund.): 397 $[M + H]^+$ (100); Anal. Calcd. ($C_{20}H_{16}ClF_3O_3$): C, 60.54; H, 4.06%. Found: C, 60.49; H, 3.93%.

*4.1.3.9. 2-(4-(3-(Trifluoromethoxy)phenoxy)phenyl)-4H-chromen-4-one (**6g**).* Yellow solid; 37%; mp 86–87 °C; ^{1}H NMR ($CDCl_3$, 400 MHz) δ 6.81 (1H, s, Ar–*H*3); 6.99–7.10 (3H, m, Ar–*H*); 7.18 (2H, d, J = 8.8, Ar–*H*); 7.41–7.48 (2H, m, Ar–*H*); 7.59 (1H, d, J = 7.6 Hz, Ar–*H*); 7.73 (1H, ddd, J = 8.6, 7.2 and 1.6 Hz, Ar–*H*); 7.96 (2H, d, J = 8.8 Hz, Ar–*H*); 8.26 (1H, dd, J = 7.6 and 1.6 Hz, Ar–*H*); ^{13}C NMR ($CDCl_3$, 101 MHz) δ 107.1; 112.6; 116.5; 117.7; 118.0; 118.4; 118.9; 123.9; 125.3; 125.8; 127.1; 128.3; 130.6; 130.9; 133.8; 156.2; 157.0; 159.6; 162.8; 178.4; IR (film): ν_{max} 1632; 1587; 1478; 1370; 1262; 1172 cm^{-1}; ESI-MS m/z (abund.): 399 $[M + H]^+$ (100); Anal. Calcd. ($C_{22}H_{13}F_3O_4$): C, 66.34; H, 3.29%. Found: C, 66.40; H, 3.22%.

*4.1.3.10. 3-(4-Bromophenyl)-4H-chromen-4-one (**6j**).* white solid; 25%; mp 179–181 °C; ^{1}H NMR ($CDCl_3$, 400 MHz) δ 6.80 (1H, s, Ar–*H*3); 7.43 (1H, td, J = 8.0 and 1.0 Hz, Ar–*H*); 7.56 (1H, d, J = 8.0 Hz, Ar–*H*); 7.67 (2H, d, J = 8.8 Hz, Ar–*H*); 7,71 (1H, ddd, J = 8.4, 7.2 and 1.6 Hz, Ar–*H*); 7.80 (2H, d, J = 8.8 Hz, Ar–*H*); 8.23 (1H, dd, J = 8.0 and 1.6 Hz, Ar–*H*); ^{13}C NMR ($CDCl_3$, 101 MHz) δ 107.8; 118.2; 124.0; 125.5; 125.9; 126.4; 127.8; 130.8; 132.5; 134.1; 156.3; 162.4; 178.4; IR (film): ν_{max} 1640; 1468; 1406; 1130; 752 cm^{-1}; ESI-MS m/z (abund.): 303 $[M + H]^+$ (100); Anal. Calcd. ($C_{15}H_9BrO_2 \cdot 0.5H_2O$): C, 58.09; H, 3.26%. Found: C, 58.24; H, 3.12%.

*4.1.3.11. 2-([1,1′-Biphenyl]-4-yl)-3-bromo-7-bromomethyl-6-chloro-4H-chromen-4-one (**6k**).* Compound **6i** (1 M eq.), NBS (1.2 M eq.) and benzoyl peroxide (0.1 M eq.) were suspended in CCl_4 (5 mL/mmol). The mixture was heated to reflux for 24 h and then cooled to room temperature. The organic phase was washed with water and evaporated to dryness *in vacuum*. The crude product was purified by flash chromatography, hexane : EtOAc (9:1). Yellow solid; 27%; mp 262–265 °C; ^{1}H NMR ($CDCl_3$, 400 MHz) δ 4.67 (2H, s, C*H*$_2$); 7.45 (1H, t, J = 7.0 Hz, Ar–*H*); 7.53 (2H, t, J = 7.4 Hz, Ar–*H*); 7.69–7.71 (3H, m, Ar–*H*); 7.79 (2H, d, J = 8.6 Hz, Ar–*H*); 7.99 (2H, d, J = 8.6 Hz, Ar–*H*); 8.34 (1H, s, Ar–*H*); ^{13}C NMR ($CDCl_3$, 101 MHz) δ 29.0; 109.1; 120.6; 122.4; 127.1; 127.3; 127.4; 128.3; 129.0; 129.9; 131.0; 131.5; 139.7; 141.8; 144.3; 153.9; 162.2; 171.9; IR (film): ν_{max} 1651; 1613; 1549; 1453; 1409; 1332; 1076 cm^{-1}; ESI-MS m/z (abund.): 503 $[M + H]^+$ (25); 505 $[M+3]^+$ (100); Anal. Calcd. ($C_{22}H_{13}Br_2ClO_2$): C, 52.37; H, 2.60%. Found: C, 52.01; H, 2.51%.

*4.1.3.12. 2-([1,1′-Biphenyl]-4-yl)-3-bromo-6-chloro-7-methyl-4H-chromen-4-one (**6l**).* Compound **6i** (1 M eq.), NBS (1.2 M eq.) and $ZrCl_4$ (0.1 M eq.) were suspended in CH_2Cl_2. The suspension was stirred at room temperature for 24 h and water was added. The aqueous phase was extracted with CH_2Cl_2 (4 × 50 mL), and the combined extracts were evaporated to dryness under reduced pressure. The crude product was purified by flash chromatography, hexane : EtOAc (9:1). Yellow solid; 10%; mp 190–192 °C; ^{1}H NMR ($CDCl_3$, 400 MHz) δ 2.55 (3H, s, C*H*$_3$); 7.41–7.48 (2H, m, Ar–*H*); 7.52 (2H, t, J = 7.6 Hz, Ar–*H*); 7.66–7.72 (2H, m, Ar–*H*); 7.78 (2H, d, J = 8.6 Hz, Ar–*H*); 7.97 (2H, d, J = 8.6 Hz, Ar–*H*); 8.28 (1H, s, Ar–*H*); ^{13}C NMR ($CDCl_3$, 101 MHz) δ 21.0; 109.0; 119.7; 120.8; 126.0; 127.0; 127.3; 128.2; 129.0; 129.9; 131.4; 132.5; 139.8; 143.7; 144.1; 153.9; 161.7; 172.1; IR (film): ν_{max} 1651; 1606; 1542; 1409 cm^{-1}; HRMS calc. ($C_{22}H_{14}BrClO_2$): 423.9866/425.9845. Found: 423.9861/425.9839.

*4.1.4. General Suzuki coupling for the preparation of flavones **6m–r***

To a solution of compound **6i** in dry 1,4-dioxane at room temperature was consecutively added $PdCl_2(Ph_3P)_2$ (0.1 equiv.), Na_2CO_3 1 N (3 equiv.), and boronic acid (1.2 equiv.). After degassing during 5 min, the resulting mixture was heated at 100 °C, under N_2 atmosphere, during 3–5 h. The mixture was then cooled to room temperature, diluted with DCM and filtered through a pad of celite. The filtrate was concentrated under reduce pressure and the crude product was purified by flash chromatography (hexane:EtOAc, 8:2) or thin layer chromatography (EtOAc:hexane:Et_3N, 6:4:0.5).

*4.1.4.1. 2-([1,1′-Biphenyl]-4-yl)-4H-chromen-4-one (**6m**).* White solid; 75%; mp 135–137 °C; ^{1}H NMR ($CDCl_3$, 400 MHz) δ 6.88 (1H, s, Ar–*H*3); 7.38–7.46 (2H, m, Ar–*H*); 7.49 (2H, t, J = 7.5 Hz, Ar–*H*); 7.60 (1H, d, J = 8.4 Hz, Ar–*H*); 7.66 (2H, d, J = 7.5 Hz, Ar–*H*); 7.69–7.78 (3H, m, Ar–*H*); 8.02 (2H, d, J = 8.5 Hz, Ar–*H*); 8.25 (1H, dd, J = 7.9 and 1.3 Hz, Ar–*H*); ^{13}C NMR ($CDCl_3$, 101 MHz) δ 107.6; 118.2; 124.1; 125.4; 125.9; 126.9; 127.3; 127.8; 128.4; 129.2; 130.6; 133.9; 139.9; 144.6; 156.4; 163.3; 178.6; IR (film): ν_{max} 1645; 1574; 1464; 1409; 1243 cm^{-1}; ESI-MS m/z (abund.): 299 $[M + H]^+$ (100); Anal. Calcd. ($C_{21}H_{14}O_2 \cdot 1.9H_2O$): C, 75.84; H, 5.41%. Found: C, 75.94; H, 5.74%.

*4.1.4.2. 2-(4′-Chloro-[1,1′-biphenyl]-4-yl)-4H-chromen-4-one (**6n**).* White solid; 50%; mp 208–210 °C; ^{1}H NMR ($CDCl_3$, 400 MHz) δ 6.88 (1H, s, Ar–*H*3); 7.41–7.49 (3H, m, Ar–*H*); 7.56–7.63 (3H, m, Ar–*H*);

7.69–7.76 (3H, m, Ar–*H*); 8.02 (2H, d, J = 8.6 Hz, Ar–*H*); 8.25 (1H, dd, J = 7.9 and 1.5 Hz, Ar–*H*); ^{13}C NMR ($CDCl_3$, 101 MHz) δ 107.7; 118.2; 124.2; 125.5; 125.9; 127.0; 127.7; 128.5; 129.4; 131.0; 134.0; 134.6; 138.3; 143.2; 156.4; 163.1; 178.6; IR (film): ν_{max} 1651; 1466; 1371; 1130; 810 cm^{-1}; ESI-MS m/z (abund.): 333 $[M + H]^+$ (100); HRMS (ESI) m/z calcd. for $[C_{21}H_{14}ClO_2]^+$: 333.06768 $[M + H]^+$; found: 333.06777.

*4.1.4.3. 2-(4′-Fluoro-[1,1′-biphenyl]-4-yl)-4H-chromen-4-one (**6o**).* White solid; 64%; mp 182–184 °C; ^{1}H NMR ($CDCl_3$, 400 MHz) δ 6.87 (1H, s, Ar–*H*3); 7.17 (2H, t, J = 8.7 Hz, Ar–*H*); 7.43 (1H, td, J = 8.0 and 1.0 Hz, Ar–*H*); 7.56–7.64 (3H, m, Ar–*H*); 7.67–7.75 (3H, m, Ar–*H*); 8.00 (2H, d, J = 8.6 Hz, Ar–*H*); 8.24 (1H, dd, J = 8.0 Hz, 1.5 Hz, Ar–*H*); ^{13}C NMR ($CDCl_3$, 101 MHz) δ 107.6; 116.1; 118.2; 124.1; 125.4; 125.8; 126.9; 127.6; 128.9; 130.6; 134.0; 136.0; 143.5; 156.4; 162.5; 164.3; 178.6; IR (film): ν_{max} 1638; 1472; 1402; 1364; 1243; 822 cm^{-1}; ESI-MS m/z (abund.): 317 $[M + H]^+$ (100); Anal. Calcd. ($C_{21}H_{13}FO_2 \cdot 3.4H_2O$): C, 66.79; H, 5.30%. Found: C, 67.08; H, 5.70%.

*4.1.4.4. 4′-(4-Oxo-4H-chromen-2-yl)-[1,1′-biphenyl]-4-carbaldehyde (**6p**).* White solid; 80%; mp 218–220 °C; ^{1}H NMR ($CDCl_3$, 400 MHz) δ 6.89 (1H, s, Ar–*H*3); 7.44 (1H, t, J = 7.6 Hz, Ar–*H*); 7.60 (1H, d, J = 8.4 Hz, Ar–*H*); 7.72 (1H, t, J = 8.4 Hz, Ar–*H*); 7.79 (2H, d, J = 8.0 Hz, Ar–*H*); 7.81 (2H, d, J = 8.4 Hz, Ar–*H*); 8.00 (2H, d, J = 8.0 Hz, Ar–*H*), 8.04 (2H, d, J = 8.4 Hz, Ar–*H*); 8.24 (1H, d, J = 7.6 Hz, Ar–*H*); 10.10 (1H, s, *CH*O); ^{13}C NMR ($CDCl_3$, 101 MHz) δ 107.9; 118.2; 124.1; 125.5; 125.9; 127.1; 127.9; 128.1; 130.5; 131.8; 134.1; 135.9; 142.9; 145.7; 156.4; 162.8; 178.5; 191.9; IR (film): ν_{max} 2918; 2749; 1705; 1640; 1466; 1377; 1128; 817 cm^{-1}; ESI-MS m/z (abund.): 327 $[M + H]^+$ (100); Anal. Calcd. ($C_{22}H_{14}O_3 \cdot 1.2H_2O$): C, 75.93; H, 4.76%. Found: C, 75.93; H, 4.66%.

*4.1.4.5. 2-(4-(6-Aminopyridin-3-yl)phenyl)-4H-chromen-4-one (**6q**).* Yellow solid; 42%; mp 244–246 °C; ^{1}H NMR ($CDCl_3$, 400 MHz) δ 4.65 (2H, br. s, N*H*$_2$); 6.62 (1H, d, J = 8.6 Hz, Ar–*H*); 6.86 (1H, s, Ar–*H*3); 7.43 (1H, td, J = 8.0 and 1.0 Hz, Ar–*H*); 7.59 (1H, d, J = 8.0 Hz, Ar–*H*); 7.67 (2H, d, J = 8.5 Hz, Ar–*H*); 7.69–7.76 (2H, m, Ar–*H*); 7.99 (2H, d, J = 8.5 Hz, Ar–*H*); 8.25 (1H, dd, J = 8.0 and 1.6 Hz, Ar–*H*); 8.40 (1H, d, J = 2.1 Hz, Ar–*H*); ^{13}C NMR ($CDCl_3$, 101 MHz) δ 107.5; 108.8; 118.2; 124.2; 125.4; 125.9; 126.3; 126.7; 127.1; 130.2; 133.9; 136.6; 141.7; 146.7; 156.4; 158.3; 163.3; 178.6; IR (film): ν_{max} 2920, 1634, 1593, 1385, 1128 cm^{-1}; ESI-MS m/z (abund.): 315 $[M + H]^+$ (100); Anal. Calcd. ($C_{20}H_{14}N_2O_2 \cdot 0.6H_2O$): C, 73.87 H, 4.72; N, 8.62%. Found: C, 73.99; H, 4.65; N, 8.25%.

*4.1.4.6. 2-(4-(Quinolin-3-yl)phenyl)-4H-chromen-4-one (**6r**).* White solid; 82%; mp 211–213 °C; ^{1}H NMR ($CDCl_3$, 400 MHz) δ 6.91 (1H, s, Ar–*H*3); 7.45 (1H, td, J = 8.0 and 0.8 Hz, Ar–*H*); 7.59–7.65 (2H, m, Ar–*H*); 7.70–7.80 (2H, m, Ar–*H*); 7.89 (2H, d, J = 8.5 Hz, Ar–*H*); 7.92 (1H, d, J = 8.4 Hz, Ar–*H*); 8.10 (2H, d, J = 8.5 Hz, Ar–*H*); 8.17 (1H, d, J = 8.5 Hz, Ar–*H*); 8.26 (1H, dd, J = 8.0 and 1.5 Hz, Ar–*H*); 8.39 (1H, d, J = 2.4 Hz, Ar–*H*); 9.23 (1H, d, J = 2.4 Hz, Ar–*H*); ^{13}C NMR ($CDCl_3$, 101 MHz) δ 107.9; 118.2; 124.2; 125.5; 125.9; 127.2; 127.5; 128.0; 128.1; 128.3; 129.5; 130.1; 131.5; 132.6; 133.7; 134.0; 141.2; 147.8; 149.5; 156.4; 162.9; 178.5; IR (film): ν_{max} 1634; 1574; 1464; 1408; 1373; 1128; 833 cm^{-1}; ESI-MS m/z (abund.): 350 $[M + H]^+$ (100); Anal. Calcd. ($C_{24}H_{15}NO_2 \cdot 0.7H_2O$): C, 79.63; H, 4.58; N, 3.87%. Found: C, 79.73; H, 4.36; N, 3.79%.

4.2. Biology

4.2.1. Blood stage infection measurements

Human red blood cells infected with *P. falciparum* strain W2 at ~1% parasitemia and synchronized with 5% sorbitol, were incubated with test compounds in 96-well plates at 37 °C for 48 h, beginning at the ring stage, in RPMI-1640 medium, supplemented with 25 mM HEPES pH 7.4, 10% heat inactivated human serum (or 0.5% Albumax/2% human serum), and 100 μM Hypoxanthine, under an atmosphere of 3% O_2, 5% CO_2, 91% N_2. After 48 h the cells were fixed in 2% HCHO in PBS; transferred into PBS with 100 mM NH_4Cl, 0.1% Triton X-100, 1 nM YOYO-1; and analyzed in a flow cytometer (FACSort, Beckton Dickinson; EX 488 nm, EM 520 nm). IC_{50} values were calculated using GraphPad Prism software.

4.2.2. Liver stage infection measurements

Huh-7 cells, a human hepatoma cell line, were cultured in RPMI 1640 medium supplemented with 10% v/v fetal calf serum (FCS), 1% v/v non-essential amino acids, 1% v/v penicillin/streptomycin, 1% v/v glutamine and 10 mM 4-(2-hydroxyethyl)-1-piperazine-ethanesulphonic acid (HEPES), pH 7, and maintained at 37 °C with 5% CO_2. To measure inhibition of liver stage infection, a firefly luciferase-expressing *P. berghei* line, *Pb*GFP-Luc$_{con}$, was employed, as previously described [46]. Inhibition of parasite development was measured when the compounds were added 1 h before the infection of Huh-7 cells and infection was measured 48 h after sporozoite addition. The effect of the compounds on the viability of Huh-7 cells was assessed by the AlamarBlue assay (Invitrogen, UK), using the manufacturer's protocol. Non-linear regression analysis was used to fit the normalized results of the dose-response curves, and IC_{50} values were determines using the SigmaPlot software.

4.2.3. In vitro cytotoxicity assessment in HepG2 cells

HepG2 cells (a human hepatoma cell line), cultured in DMEM medium supplemented with 10% v/v fetal calf serum (FCS), 1% v/v non-essential amino acids, 1% v/v penicillin/streptomycin, 1% v/v glutamine and 10 mM 4-(2-hydroxyethyl)-1-piperazineethane-sulphonic acid (HEPES), pH 7, and maintained at 37 °C with 5% CO_2, were incubated with each compound at varying concentrations for a period of 48 h in 96-well plates (10,000 cells/well). After this period, the effect of the compounds on the viability of HepG2 cells was assessed by the AlamarBlue assay (Invitrogen, UK), using the manufacturer's protocol.

4.3. Docking studies

The bc_1 complex crystallographic structure was obtained from the RCSB Protein Data Bank (PDB code 3CX5) [33]. Bound inhibitors and other coordinated molecules were removed from the PDB file. All crystallized water molecules were also removed, except when a catalytic water molecule was used in the docking calculations. The protonation states of the residues were assigned using the Protonate 3D algorithm within the Molecular Operating Environment (MOE) 2012.10 program (www.chemcomp.com). Only the polar hydrogen atoms were kept, and the protonated state of His^{181} was assigned for each docking experiments. The 3D molecular structures of the docked molecules were built, parameterized, and energy minimized with MOE using the MMFF94x force field. AutoDock 4.0 was chosen for the docking calculations within the DOVIS 2.0 package [48]. The grid box was set with 40 points in the x and y and 44 in the z direction. The default value of 0.375 Å for spacing between grid points was used, leading to a box size of 15 Å in x and y and 16.5 Å in z, allowing the crystallographic pose of stigmatellin to be in the middle of the box. The Lamarckian genetic algorithm conformational search with a population size of 150, 250,000 energy evaluations and a maximum of 27,000 generations per run, were used. 200 docking runs were applied in all calculations. The docking results were ranked using the AD 4.0 scoring function, and PyMOL 1.23r3pre (www.pymol.org) was used for visual inspection of the docking results.

Acknowledgments

This work was funded by Fundação para a Ciência e Tecnologia (FCT, Portugal) through projects PTDC/SAU-FCT/098734/2008 and PRDC/SAU-MIC/117060/2010. T.R., A.S.R., F.P.C. and M.P.C. acknowledge FCT for grants SFRH/BD/30689/2006, SFRH/BPD/64859/2009, SFRH/BPD/64539/2010, and SFRH/BD/61611/2009 respectively. P.J.R. is a Doris Duke Charitable Foundation Distinguished Clinical Scientist.

References

[1] Y.L. Bennani, Drug discovery in the next decade: innovation needed ASAP, Drug Discov. Today 16 (2011) 779–792.
[2] T. Rodrigues, R. Moreira, F. Lopes, New hope in the fight against malaria? Future Med. Chem. 3 (2011) 1–3.
[3] WHO, World Malaria Report, 2011. Geneva, Switzerland.
[4] M. Prudêncio, A. Rodriguez, M.M. Mota, The silent path to thousands of merozoites: the Plasmodium liver stage, Nat. Rev. Microbiol. 4 (2006) 849–856.
[5] N. Vale, R. Moreira, P. Gomes, Primaquine revisited six decades after its discovery, Eur. J. Med. Chem. 44 (2009) 937–953.
[6] S. Ganesan, B.L. Tekwani, R. Sahu, L.M. Tripathi, L.A. Walker, Cytochrome P-450-dependent toxic effects of primaquine on human erythrocytes, Toxicol. Appl. Pharmacol. 241 (2009) 14–22.
[7] A.P. Singh, N. Surolia, A. Surolia, Triclosan inhibit the growth of the late liver-stage of Plasmodium, IUBMB Life 61 (2009) 923–928.
[8] Y. Min, T.R.S. Kumar, L.J. Nkrumah, A. Coppi, S. Retzlaff, C.D. Li, B.J. Kelly, P.A. Moura, V. Lakshmanan, J.S. Freundlich, J.C. Valderramos, C. Vilcheze, M. Siedner, J.H.C. Tsai, B. Falkard, A.B.S. Sidhu, L.A. Purcell, P. Gratraud, L. Kremer, A.P. Waters, G. Schiehser, D.P. Jacobus, C.J. Janse, A. Ager, W.R. Jacobs, J.C. Sacchettini, V. Heussler, P. Sinni, D.A. Fidock, The fatty acid biosynthesis enzyme FabI plays a key role in the development of liver-stage malarial parasites, Cell Host Microb. 4 (2008) 567–578.
[9] B. Pérez, C. Teixeira, I.S. Albuquerque, J. Gut, P.J. Rosenthal, J.R.B. Gomes, M. Prudêncio, P. Gomes, *N*-cinnamoylated chloroquine analogues as dual-stage antimalarial leads, J. Med. Chem. 56 (2013) 556–567.
[10] T.N. Wells, J.N. Burrows, J.K. Baird, Targeting the hypnozoite reservoir of *Plasmodium vivax*: the hidden obstacle to malaria elimination, Trends Parasitol. 26 (2010) 145–151.
[11] P.L. Alonso, G. Brown, M. Arevalo-Herrera, F. Binka, C. Chitnis, F. Collins, O.K. Doumbo, B. Greenwood, B.F. Hall, M.M. Levine, K. Mendis, R.D. Newman, C.V. Plowe, M.H. Rodriguez, R. Sinden, L. Slutsker, M. Tanner, A research agenda to underpin malaria eradication, PLoS Med. 8 (2011) e1000406.
[12] The malERA Consultive Group on Drugs, A research agenda for malaria eradication: drugs, PLoS Med. 8 (2011) e1000402.
[13] T. Rodrigues, F. Lopes, R. Moreira, Inhibitors of the mitochondrial electron transport chain and de novo pyrimidine biosynthesis as antimalarials: the present status, Curr. Med. Chem. 17 (2010) 929–956.
[14] F.P. da Cruz, C. Martin, K. Buchholz, M.J. Lafuente-Monasterio, T. Rodrigues, B. Sonnichsen, R. Moreira, F.J. Gamo, M. Marti, M.M. Mota, M. Hannus, M. Prudêncio, Drug screen targeted at Plasmodium liver stages identifies a potent multistage antimalarial drug, J. Infect. Dis. 205 (2012) 1278–1286.
[15] R. Cowley, S. Leung, N. Fisher, M. Al-Helal, N.G. Berry, A.S. Lawrenson, R. Sharma, A.E. Shone, S.A. Ward, G.A. Biagini, P.M. O'Neill, The development of quinolone esters as novel antimalarial agents targeting the Plasmodium falciparum bc_1 protein complex, Med. Chem. Commun. 3 (2012) 39–44.
[16] Y.Q. Zhang, J.A. Clark, M.C. Connelly, F.Y. Zhu, J.K. Min, W.A. Guiguemde, A. Pradhan, L. Iyer, A. Furimsky, J. Gow, T. Parman, F. El Mazouni, M.A. Phillips, D.E. Kyle, J. Mirsalis, R.K. Guy, Lead optimization of 3-carboxyl-4(1*H*)-quinolones to deliver orally bioavailable antimalarials, J. Med. Chem. 55 (2012) 4205–4219.
[17] C. Pidathala, R. Amewu, B. Pacorel, G.L. Nixon, P. Gibbons, W.D. Hong, S.C. Leung, N.G. Berry, R. Sharma, P.A. Stocks, A. Srivastava, A.E. Shone, S. Charoensutthivarakul, L. Taylor, O. Berger, A. Mbekeani, A. Hill, N.E. Fisher, A.J. Warman, G.A. Biagini, S.A. Ward, P.M. O'Neill, Identification, design and biological evaluation of bisaryl quinolones targeting *Plasmodium falciparum* Type II NADH: quinone oxidoreductase (PfNDH2), J. Med. Chem. 55 (2012) 1831–1843.
[18] A.N. LaCrue, F.E. Saenz, R.M. Cross, K.O. Udenze, A. Monastyrskyi, S. Stein, T.S. Mutka, R. Manetsch, D.E. Kyle, 4(1H)-Quinolones with liver stage activity against Plasmodium berghei, Antimicrob. Agents Chemother. 57 (2013) 417–424.
[19] T. Rodrigues, F.P. da Cruz, M.J. Lafuente-Monasterio, D. Gonçalves, A.S. Ressurreicão, A.R. Sitoe, M.R. Bronze, J. Gut, G. Schneider, M.M. Mota, P.J. Rosenthal, M. Prudêncio, F.-J. Gamo, F. Lopes, R. Moreira, Quinolin-4(1*H*)-imines are potent antiplasmodial drugs targeting the liver stage of malaria, J. Med. Chem. 56 (2013) 4811–4815.
[20] T. Rodrigues, M. Prudêncio, R. Moreira, M.M. Mota, F. Lopes, Targeting the liver stage of malaria parasites: a yet unmet goal, J. Med. Chem. 55 (2012) 995–1012.
[21] A. Nilsen, A.N. Lacrue, K.L. White, I.P. Forquer, R.M. Cross, J. Marfurt, M.W. Mather, M.J. Delves, D.M. Shackleford, F.E. Saenz, J.M. Morrisey, J. Steuten, T. Mutka, Y. Li, G. Wirjanata, E. Ryan, S. Duffy, J.X. Kelly, B.F. Sebayang, A.M. Zeeman, R. Noviyanti, R.E. Sinden, C.H. Kocken, R.N. Price, V.M. Avery, I. Angulo-Barturen, M.B. Jimenez-Diaz, S. Ferrer, E. Herreros, L.M. Sanz, F.J. Gamo, I. Bathurst, J.N. Burrows, P. Siegl, R.K. Guy, R.W. Winter, A.B. Vaidya, S.A. Charman, D.E. Kyle, R. Manetsch, M.K. Riscoe, Quinolone-3-diarylethers: a new class of antimalarial drug, Sci. Transl. Med. 5 (2013) 177ra137.
[22] G.A. Biagini, N. Fisher, A.E. Shone, M.A. Mubaraki, A. Srivastava, A. Hill, T. Antoine, A.J. Warman, J. Davies, C. Pidathala, R.K. Amewu, S.C. Leung, R. Sharma, P. Gibbons, D.W. Hong, B. Pacorel, A.S. Lawrenson, S. Charoensutthivarakul, L. Taylor, O. Berger, A. Mbekeani, P.A. Stocks, G.L. Nixon, J. Chadwick, J. Hemingway, M.J. Delves, R.E. Sinden, A.M. Zeeman, C.H.M. Kocken, N.G. Berry, P.M. O'Neill, S.A. Ward, Generation of quinolone antimalarials targeting the *Plasmodium falciparum* mitochondrial respiratory chain for the treatment and prophylaxis of malaria, Proc. Natl. Acad. Sci. U.S.A. 109 (2012) 8298–8303.
[23] G. Auffret, M. Labaied, F. Frappier, P. Rasoanaivo, P. Grellier, G. Lewin, Synthesis and antimalarial evaluation of a series of piperazinyl flavones, Bioorg. Med. Chem. Lett. 17 (2007) 959–963.
[24] K. Kaur, M. Jain, T. Kaur, R. Jain, Antimalarials from nature, Bioorg. Med. Chem. 17 (2009) 3229–3256.
[25] F.-J. Gamo, L.M. Sanz, J. Vidal, C.d. Cozar, E. Alvarez, J.-L. Lavandera, D.E. Vanderwall, D.V.S. Green, V. Kumar, S. Hasan, J.R. Brown, C.E. Peishoff, L.R. Cardon, J.F. Garcia-Bustos, Thousands of chemical starting points for antimalarial lead identification, Nature 465 (2010) 305–310.
[26] M. Cunha-Rodrigues, S. Portugal, M. Prudêncio, L.A. Gonçalves, C. Casalou, D. Buger, R. Sauerwein, W. Haas, M.M. Mota, Genistein-supplemented diet decreases malaria liver infection in mice and constitutes a potential prophylactic strategy, PLoS One 3 (2008) e2732.
[27] C.L. Yeates, J.F. Batchelor, E.C. Capon, N.J. Cheesman, M. Fry, A.T. Hudson, M. Pudney, H. Trimming, J. Woolven, J.M. Bueno, J. Chicharro, E. Fernandez, J.M. Fiandor, D. Gargallo-Viola, F.G. de las Heras, E. Herreros, M.L. Leon, Synthesis and structure–activity relationships of 4-pyridones as potential antimalarials, J. Med. Chem. 51 (2008) 2845–2852.
[28] T. Rodrigues, R.C. Guedes, D.J.V.A. dos Santos, M. Carrasco, J. Gut, P.J. Rosenthal, R. Moreira, F. Lopes, Design, synthesis and structure-activity relationships of (1*H*-pyridin-4-ylidene)amines as potential antimalarials, Bioorg. Med. Chem. Lett. 19 (2009) 3476–3480.
[29] R.W. Winter, J.X. Kelly, M.J. Smilkstein, R. Dodean, G.C. Bagby, R.K. Rathbun, J.I. Levin, D. Hinrichs, M.K. Riscoe, Evaluation and lead optimization of antimalarial acridones, Exp. Parasitol. 114 (2006) 47–56.
[30] S. Bolgunas, D.A. Clark, W.S. Hanna, P.A. Mauvais, S.O. Pember, Potent inhibitors of the Qi site of the mitochondrial respiration complex III, J. Med. Chem. 49 (2006) 4762–4766.
[31] M.P. Carrasco, J. Gut, T. Rodrigues, M.H.L. Ribeiro, F. Lopes, P.J. Rosenthal, R. Moreira, D.J.V.A. dos Santos, Exploring the molecular basis of Q_o bc_1 complex inhibitors activity to find novel antimalarials hits, Mol. Inf. 32 (2013) 659–670.
[32] P. Hill, J. Kessl, N. Fisher, S. Meshnick, B.L. Trumpower, B. Meunier, Recapitulation in *Saccharomyces cerevisiae* of cytochrome b mutations conferring resistance to atovaquone in *Pneumocystis jiroveci*, Antimicrob. Agents Chemother. 47 (2003) 2725–2731.
[33] S.R.N. Solmaz, C. Hunte, Structure of complex III with bound cytochrome c in reduced state and definition of a minimal core interface for electron transfer, J. Biol. Chem. 283 (2008) 17542–17549.
[34] E. Darrouzet, M. Valkova-Valchanova, C.C. Moser, P.L. Dutton, F. Daldal, Uncovering the [$2Fe_2S$] domain movement in cytochrome bc1 and its implications for energy conversion, Proc. Natl. Acad. Sci. U.S.A. 97 (2000) 4567–4572.
[35] U. Brandt, U. Haase, H. Schägger, G. v. Jagow, Significance of the "Rieske" iron–sulfur protein for formation and function of the ubiquinol-oxidation pocket of mitochondrial cytochrome c reductase (bc1 complex), J. Biol. Chem. 266 (1991) 19958–19964.
[36] M.D. Esposti, S.D. Vries, M. Crimi, A. Ghelli, T. Patarnello, A. Meyer, Mitochondrial cytochrome b: evolution and structure of the protein, Biochim. Biophys. Acta 1143 (1993) 243–271.
[37] T. Rodrigues, D.J.V.A. dos Santos, R. Moreira, F. Lopes, R.C. Guedes, A quantum mechanical study of novel potential inhibitors of cytochrome bc_1 as antimalarial compounds, Int. J. Quantum Chem. 111 (2011) 1196–1297.
[38] R. Prihod'ko, M. Sychev, I. Kolomitsyn, P.J. Stobbelaar, E.J.M. Hensen, R.A. van Santen, Layered double hydroxides as catalysts for aromatic nitrile hydrolysis, Microporous Mesoporous Mater. 56 (2002) 241–255.
[39] C. Riva, C. DeToma, L. Donadel, C. Boi, R. Pennini, G. Motta, A. Leonardi, New DBU (1,8-diazabicyclo[5.4.0]undec-7-ene) assisted one-pot synthesis of 2,8-disubstituted 4*H*-1-benzopyran-4-ones, Synthesis 1997 (1997) 195–201.
[40] K. Shibatomi, Y. Zhang, H. Yamamoto, Lewis acid catalyzed benzylic bromination, Chem. Asian J. 3 (2008) 1581–1584.
[41] A. Semenov, J.E. Olson, P.J. Rosenthal, Antimalarial synergy of cysteine and aspartic protease inhibitors, Antimicrob. Agents Chemother. 42 (1998) 2254–2258.
[42] S.S. Lim, H.S. Kim, D.U. Lee, In vitro antimalarial activity of flavonoids and chalcones, Bull. Korean Chem. Soc. 28 (2007) 2495–2497.

[43] A.L. Hopkins, C.R. Groom, A. Alex, Ligand efficiency: a useful metric for lead selection, Drug Discov. Today 9 (2004) 430–431.
[44] R. Sharma, A.S. Lawrenson, N.E. Fisher, A.J. Warman, A.E. Shone, A. Hill, A. Mbekeani, C. Pidathala, R.K. Amewu, S. Leung, P. Gibbons, D.W. Hong, P. Stocks, G.L. Nixon, J. Chadwick, J. Shearer, I. Gowers, D. Cronk, S.P. Parel, P.M. O'Neill, S.A. Ward, G.A. Biagini, N.G. Berry, Identification of novel antimalarial chemotypes via chemoinformatic compound selection methods for a high-throughput screening program against the novel malarial target, PfNDH2: increasing hit rate via virtual screening methods, J. Med. Chem. 55 (2012) 3144–3154.
[45] S. Schultes, C. de Graaf, E.E.J. Haaksma, I.J.P. de Esch, R. Leurs, O. Krämer, Ligand efficiency as a guide in fragment hit selection and optimization, Drug Discov. Today 7 (2010) e157–e162.
[46] I.H.J. Ploemen, M. Prudencio, B.G. Douradinha, J. Ramesar, J. Fonager, G.J. van Gemert, A.J.F. Luty, C.C. Hermsen, R.W. Sauerwein, F.G. Baptista, M.M. Mota, A.P. Waters, I. Que, C.W.G.M. Lowik, S.M. Khan, C.J. Janse, B.M.D. Franke-Fayard, Visualisation and quantitative analysis of the rodent malaria liver stage by real time imaging, PLoS One 4 (2009) e7881.
[47] J.S. Sawyer, E.A. Schmittling, J.A. Palkowitz, W.J. Smith, Synthesis of diaryl ethers, diaryl thioethers, and diarylamines mediated by potassium fluoride alumina and 18-crown-6: expansion of scope and utility, J. Org. Chem. 63 (1998) 6338–6343.
[48] X. Jiang, K. Kumar, X. Hu, A. Wallqvist, J. Reifman, DOVIS 2.0: an efficient and easy to use parallel virtual screening tool based on AutoDock 4.0, Chem. Cent. J. 2 (2008) 18.